Electrostatically Self-Assembled Multilayers of Chitosan and Xanthan Studied by Atomic Force Microscopy and Micro-Interferometry

Gjertrud Maurstad,[1,2] *Andreas R. Bausch,*[2] *Pawel Sikorski,*[1] *Bjørn T. Stokke**[1]

[1] Biophysics and Medical Technology, Dept. of Physics, The Norwegian University of Science and Technology, NTNU, NO-7491 Trondheim, Norway
Fax: +47 73597710; E-mail: bjorn.stokke@phys.ntnu.no
[2] Lehrstuhl für Biophysik, E22, Technische Universität München, James-Franck-Strasse 1, D-85748 Garching, Germany

Summary: The thickness and surface morphology of electrostatically self-assembled films of chitosan and xanthan (persistence length of ~120nm) have been studied using dual-wavelength Reflection Interference Contrast Microscopy (DW-RICM) and tapping mode Atomic Force Microscopy (AFM). The multilayers were prepared at two ionic strengths (5mM and 150mM). When the multilayers were assembled at 150 mM a network like morphology was observed after one bilayer. This structure was found to be of large influence in the further growth of the multilayers, with the same kind of network structure being observed at all number of bilayers. A lack of swelling behaviour, as well as the network structure and the poresize of the network, is suggested to originate from the high chain stiffness of xanthan.

Keywords: atomic force microscopy (AFM); chitosan; DW-RICM; xanthan

Introduction

Oppositely charged polyelectrolytes form complexes when mixed in solution. One important factor influencing the morphology of the complexes is the chain stiffness.[1-3] The self-assembly process leading to the formation of polyelectrolyte complexes can also be used to build thin polymer films consisting of alternating polycation and polyanion layers. The multilayers assemble due to electrostatic interaction between polyelectrolytes of opposite charge, and the assembly process is further promoted by an increased entropy due to the release of counterions.[4] The adsorption process is further enhanced by the multiplicity of segment contacts acting cooperatively.[5] The sequential adsorption of polyelectrolytes and hence the multilayer growth depend on charge reversal in each adsorption step.[6]

 DOI: 10.1002/masy.200550916

Xanthan is a stiff microbial polysaccharide with a persistence length of L_p ~120nm.[7-9] We have earlier reported that xanthan-chitosan complexes have well-defined morphologies.[10] In this study we pursue studies of this system but now restricting the degrees of freedom as compared to solution complexation by assembling multilayers at a surface. There are some reports on the fabrication of multilayers with DNA as one of the components,[11-14] but apart from this to our knowledge most polyelectrolytes commonly employed for multilayer fabrication are rather flexible (e.g. PSS, PDADMA, PAH).

The aim of the present study is to investigate basic features of chitosan-xanthan multilayer growth in terms of layer thickness and surface morphology. Taken together the observations in this study lend support to the growth and response of this multilayer system being determined by the chain stiffness of xanthan. The open multilayer structure formed, at variance with the smoother multilayer surfaces reported for more flexible polymers, indicate that the porosity of multilayer assemblies can be tuned by the selection of polymers with varying chain stiffness.

Materials and methods

Biopolymer samples

Xanthan was purified from a fermentation broth (Statoil, Bioferm) by filtration and precipitation as previously described.[10] The M_w of this sample is 5×10^6g/ml, determined by SEC-LALLS.[15] Chitosan (kindly provided by Dr. K.M.Vårum, Dept. of Biotechnology, NTNU) with an average degree of acetylation F_A = 0.1, weight average molecular weight M_w= 33×10^3g/mol, and intrinsic viscosity [η] = 210ml/g was employed. The chitosan was dissolved in acetic acid (1%), to a concentration of 1mg/ml.

Preparation of polyelectrolyte multilayers

The deposition substrates (mica slides or glass cover slides) used for preparing samples for AFM imaging, were first cleaned by immersing the mica or glass in 50%methanol and 50%HCl for 30minutes, followed by rinsing in MQ-water.[16] The slides were then dried in a stream of N_2 before the build-up of the multilayers. For height measurements with DW-RICM, glass cover slides were cleaned by sonication twice in 2% Hellmanex solution (Hellma, Germany) for 30minutes, followed by sonication twice in MQ-water. Between each sonication, the glass slides were rinsed extensively in MQ-water. The polyelectrolyte multilayers were prepared by manual immersion in alternating polycation and polyanion solutions (50μg/ml), with the standard immersion time being 5minutes. The build-up was

carried out at two different ionic strengths (5mM and 150mM NH_4Ac; both at pH 5.5). Between each polyelectrolyte exposure, the sample was rinsed three times in aqueous salt solution of the same ionic strength as that used in the polymer solution. For AFM-imaging, the samples were dried in a stream of N_2 after polyelectrolyte deposition, followed by vacuum drying at 1.3×10^{-4} Pa for at least 4 hours. In the following the notation $(chit\_xan)_n$ is adapted, with n being the number of bilayers (BL). Upon drying, NaCl forms salt crystals in the samples, introducing obscuring effects during AFM imaging. Thus, ammonium acetate (NH_4Ac) was preferred for adjustment of ionic strength, and used for both determination of surface morphology using AFM and film thickness employing DW-RICM. However, polyelectrolyte film thickness measurements with DW-RICM showed that there was no height difference in samples prepared with NH_4Ac as compared to NaCl.

Atomic force microscopy.

Tapping mode AFM imaging (Digital Instruments Multimode IIIa) was carried out at ambient conditions using vacuum dried specimens.[10] The AFM height topographs were flattened line by line using the software supplied by Digital Instruments, and further image analysis was carried out in custom developed image processing software (IDL v 5.3, Research System, Inc.) as follows.

First- and second-order surface statistic parameters were extracted to characterise the surface morphology. The surface height distribution was obtained from the image height data and the root mean squared roughness R_{rms} was then calculated using equation 1.

$$R_{rms} = \sqrt{\frac{\sum(h_i - h_{ave})^2}{N}} \qquad (1)$$

where h_i is the height at point i, h_{ave} the average height within the calculation area and N the number of data points. Additionally, the height auto-correlation function was calculated from equation 2.

$$g(r) = \langle g(r_0, r)\rangle_{r_0} = \langle h(r_0)h(r_0 + r)\rangle_{r_0} - h_{ave}^2 = \langle (h(r_0) - h_{ave})(h(r_0 + r) - h_{ave})\rangle_{r_0} \qquad (2)$$

where $h(r_0)$ and $h(r_0+r)$ are the absolute values of height at positions r_0 and r_0+r . In the calculation process, an area of the image with a size r_{calc} was selected. Then for each point within this area (r_0) the function $g(r_0, r)$ for r in the range between 0 and r_{max} was calculated. The auto-correlation function $g(r)$ was then calculated by averaging $g(r_0,r)$ over all selections of r_0 within the area. The height auto-correlation function was fitted to a model function describing a random surface, the self-affine model (eq. 3):

$$g(r) = ae^{-(r/\xi)^{2\alpha}} \quad (3)$$

where a is a fitting parameter, and ξ is the correlation length. The self-affine model implies that the statistical properties of the surface is invariant to the transformation $x, y \rightarrow bx, by$ and $h \rightarrow b^{\alpha}h$, with α being the scaling-parameter between lateral and vertical dimensions, and b is a constant. Furthermore, extracting the α-parameter from the self-affine fit will also give an indication of whether the correlation function is closer to a gaussian or an exponential function since both of these are subsets of the self-affine model. Additionally, the power spectral density (PSD) was obtained as the square magnitude of the complex Fourier transform of the correlation function.

Dual Wavelength Reflection Interference Contrast Microscopy

Briefly, in RICM, monochromatic light is incident on the sample over which a probe, typically a bead, hovers. Light reflected from the glass-buffer interface and from the buffer-bead interface interferes giving rise to a characteristic pattern of Newton fringes for a spherical object. In DW-RICM interferograms are obtained simultaneously and independently at two wavelengths to enable measurement of absolute heights of the bead above the surface. The periodicity of the second wavelength together with the boundary conditions of both wavelengths (zero intensity at zero height), introduces a phase relation between the two wavelengths yielding the basis for unambiguous height determination up to ~800nm.[17] The application of this technique for film thickness measurements has previously been verified for PSS/PAH mulitlayers.[18]

The reflection interference microscope is an inverted microscope (Axiomat Zeiss) that is equipped with an antiflex objective (oil immersion, 63×, N.A. 1.3; Zeiss) in addition to the two polarizers. In the DW-RICM, the sample is illuminated by bichromatic light obtained by passing light from a 100W mercury vapour lamp through an interference filter (AF-Analysetechnik, Germany). The two wavelengths (λ=486nm and λ=546.1nm) are separated by a dichroic filter after image formation and the two images recorded independently with two CCD cameras (Hamamatsu, Japan). The images were then analysed and the height extracted by employing a user interactive software developed for this purpose.[17, 19, 20] In the height calculations, the refractive index of the layers has been approximated by the refractive index of water. However, for standard refractive indices of polyelectrolytes, the error introduced by this will be minor.

Polystyrene beads of diameter 10.15 ± 0.06μm (Duke Scientific, Palo Alta, USA) were used as probes for the RICM measurements. The beads were coated with bovine serum albumin (BSA, Sigma-Aldrich) to reduce possible hydrophobic attractions. The coating was carried out by incubation with BSA-solution (1mg/ml, 30 min) followed by washing of excess BSA by four cycles of sedimentation (4000rpm, 4min) and resuspension of the beads in MQ-water.

Results

Build-up process and swelling studies measured with DW-RICM.

The thickness of the self-assembled polyelectrolyte layers was determined employing DW-RICM. The measurements showed that when multilayers were prepared at 150mM a certain number of bilayers was necessary before stable growth conditions were achieved (Figure 1a). This finding is similar to previous reports on multilayer formation, where a few initial layers are needed to reach a regime where the adsorption process is dominated purely by the multilayer charge density.[6, 21-23] Additional measurements showed that the sample-to-sample variations in the measured height (data not shown) are of the same order as the height variations within a single sample, indicating a reproducible BL deposition process.

Contrary to the observations for the polyelectrolyte films assembled at 150 mM, no general increase in the film thickness with the number of deposited bilayers was observed for the samples prepared at I = 5 mM (Figure 1b). The film thickness for 10 and 20 BL was only slightly increased as compared to 5 BL. The films prepared at 5 mM were thicker than those prepared at 150 mM except at 20 BL.

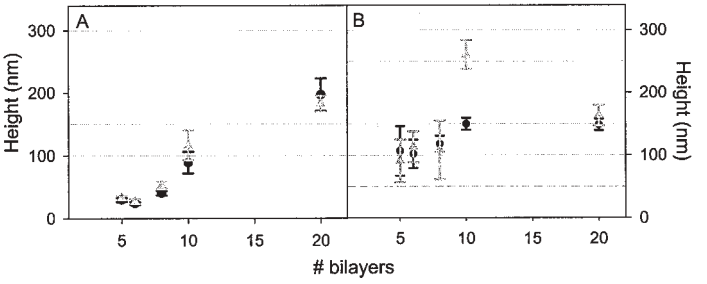

Figure 1. The thickness of chitosan-xanthan multilayers as a function of bilayers as measured with DW-RICM. a) Prepared at 150 mM and b) prepared at 5mM. The multilayers were measured at 5mM (circles) and 150mM (triangles).

The swelling response of the multilayer films was investigated by changing the ionic strength after the sample preparation (both increased from 5mM to 150mM and decreased from 150mM to 5mM for the two preparation conditions). In neither case was any change in multilayer thickness measured. A reversible swelling has been reported to occur only for a narrow range of salt concentrations.[24] Therefore, to investigate the swelling behaviour further, the thickness of a 5 BL sample prepared at 5mM was measured after equilibration in increasing ionic strength (5mM, 150mM, 300mM, and 500mM). Again, all measurements showed only small variations in the film thickness (less than the standard deviation of the mean thickness value at 5mM). In order to further characterise the multilayers, the surface morphologies of the xanthan-chitosan multilayers were studied by atomic force microscopy.

Build-up process at two ionic strengths: morphology and surface characteristics determined by AFM.

The first polyelectrolyte bilayer yielded a surface morphology independent of the ionic strength in the polymer solution (150 mM or 5 mM), both revealing a network like structure (illustrated in Figure 2a). For preparation at 150mM a network structure was observed for all number of bilayers. However at 20 BL there were additionally regions on the surface where polymer had accumulated on top of the network structure (Figure 2b). For one BL, the diameter of the network voids were typically in the range 20-50nm (diameter measured by section analysis of AFM topographs). The dimension of these voids increased in size with increasing number of BL, to 50-100 nm for 5 BL, 80-150 nm for 10 BL and further to 100-150 nm for 20 BL.

The surface morphology observed when the layers were prepared at I = 5 mM was different from the 150mM case. The AFM topographs showed two types of domains present on the surface, with a number of aggregates emerging on top of the network structure at about 5 bilayers. The underlying network structure is similar to that observed for preparation at I =150mM. When the number of bilayers is increased the aggregates increase both in lateral size and in number. Furthermore, the connections between the aggregates were thicker than the network strands (Figure 2c). The network underneath the aggregates underwent only minor changes in appearance with increasing number of BL. The diameter of the voids increased at first, before levelling off at values in the same range

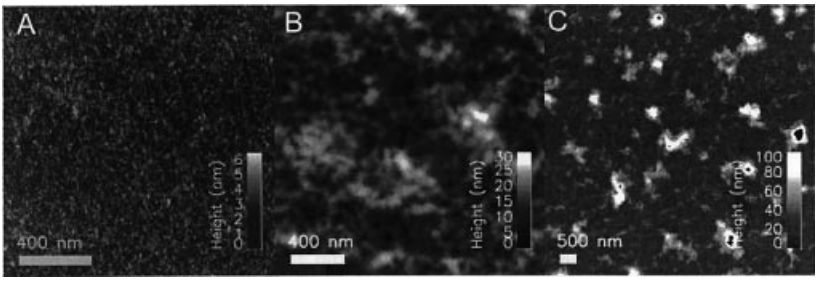

Figure 2. AFM topographs of chitosan-xanthan multilayers; a) 1 bilayer prepared at 150mM, b) 20 bilayers prepared at 150mM and c) 20 bilayers prepared at 5mM.

for all number of bilayers as for the multilayers prepared at 150mM. Even though the diameter did not increase much, the voids became easier to visualise with increasing number of BL for both preparation conditions. This feature is probably caused by a larger height-difference between the openings in the network and the surrounding network strands.

The surface roughness showed an increase with increasing number of deposited BL (Figure 3 and Table 1). This is similar to trends reported for other systems.[13, 25, 26] The high roughness for $(chit\_xan)_{20}$ prepared at I = 5mM is due to the large number of aggregates present on the surface.

Calculation of the PSD revealed that for a low number of bilayers (1 and 5) there are two regions in the log-log plot (example in Figure 4a). At low spatial frequencies (q) the PSD was constant and independent of the frequency, whereas at higher frequencies a power-law dependence was evident. The transition between these two regions is given by the transition frequency, q_{tr}.

Table 1. Roughness of (chit_xan) multilayers and the α-parameter extracted from fitting the correlation function to the self-affine model.

	Preparation conditions	Roughness (nm)[#]	α from self-affine fit[#]
$(chit\_xan)_1$	5mM	0.32 ± 0.05	0.26 ± 0.30
$(chit\_xan)_5$	5mM	2.82 ± 1.8	0.40 ± 0.25
$(chit\_xan)_{10}$	5mM	5.79 ± 1.1	0.49 ± 0.14
$(chit\_xan)_{20}$	5mM	23.66 ± 8.3	0.67 ± 0.15
$(chit\_xan)_1$	150mM	0.5 ± 0.01	0.30 ± 0.10
$(chit\_xan)_5$	150mM	1.24 ± 0.4	0.29 ± 0.10
$(chit\_xan)_{10}$	150mM	5.56 ± 3.1	0.56 ± 0.17
$(chit\_xan)_{20}$	150mM	12.19 ± 5.6	0.62 ± 0.20

[#] the values are mean ± standard deviations based on a number of AFM topographs

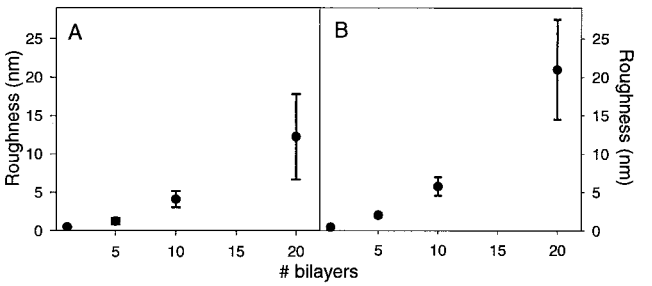

Figure 3. The surface roughness of chitosan-xanthan multilayers analysed from AFM topographs. The multilayers were a) prepared at 150mM and b) prepared at 5mM.

At dimensions corresponding to frequencies below q_{tr} there is no significant fluctuations in height. The q_{tr} was observed to shift from 0.02-0.03 nm^{-1} at one layer pair towards lower frequencies to ~ 0.01 nm^{-1} at five layer pairs for the multilayers prepared from 150mM. At 10BL the PSD was well described by one single power law within the experimental frequency window. When a low ionic strength was employed during deposition, the transition frequency decreased with number of bilayers (from ~ 0.07nm^{-1} at 1BL, ~ 0.03nm^{-1} at 5BL to 0.01-0.02 nm^{-1} at 10BL). Only at twenty bilayers was the PSD described by one power-law exponent in q over the whole experimental frequency range (Figure 4e). No systematic dependence of the PSD on the scan-size was observed. This was at variance with the correlation length ξ which was found to depend on the scan-size of the topographs, the dependence being less pronounced for preparation from 5mM salt solution than from 150mM.

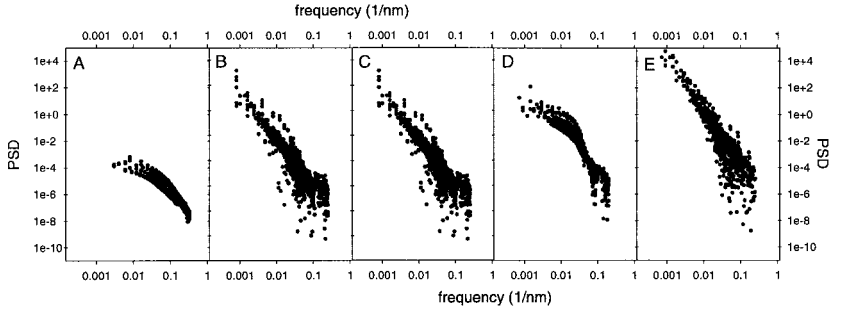

Figure 4. The power spectral density extracted from the AFM topographs of chitosan-xanthan multilayers; a) 1 bilayer at 150mM; b) 10 bilayer at 150mM; c) 20 bilayer at 150mM; d) 10 bilayer at 5mM and e) 20 bilayer at 5mM.

Discussion

In the following the observations of surface morphologies, film thickness and swelling response of the xanthan-chitosan multilayer system is explained by a model based on the behaviour of polyelectrolytes in solution. Of particular importance is that, at the conditions employed in this study, xanthan is an extended molecule, and relatively insensitive to changes in ionic strength due to its large structural persistence length of ~120 nm.[7-9]

Adsorption of the first layer of xanthan onto the chitosan layer resulted in a network-like appearance of the surface, leaving xanthan-free voids between the network strands, apparently areas without charge reversal. Further adsorption chitosan and xanthan appeared to take place preferentially along these network chains. A study of poly(allylamine) and poly(vinyl sulfate) multilayers in salt (0.1M NaCl) has shown that adsorbing polymer preferentially anchors to aggregated sites, not spreading over the whole interfacial region.[25] For the chitosan-xanthan system, selective adsorption will take place along surface heterogeneities of the network present after the first bilayer. Consequently the morphology of the initial adsorbed layer of xanthan will be dominant in determining the main morphological features of consecutive layers.

The addition of more polymer to the surface in the adsorption step has been suggested to be limited by steric interactions (excluded-volume effects of the polymer) and not the availability of surface sites.[5, 27] The presence of voids in between the network strands made up by xanthan differs from the morphology of most polyelectrolyte multilayers reported previously.[26, 28-30] It is suggested that the formation of the distinct network for the present system is due to the high rigidity of xanthan. The steric effects due to the high chain stiffness and the large radius of gyration of xanthan will increase the volume occupied by each polymer. A regular network structure has been observed also when assembling multilayers from an even stiffer polyanion than xanthan in combination with chitosan (unpublished results), supporting the view that the chain stiffness is important in determining the morphology. In the subsequent deposition steps polymer selectively adsorb along the network strands, thus accentuating the height differences on the multilayer surface with increasing number of bilayers. This was confirmed in the analysis of the AFM topographs, as the α-parameter, reflecting the relative scaling between vertical and lateral dimensions,[31] was found to increase with increasing number of bilayers (Table 1). Addtionally, the voids of the network became more pronounced for increasing number of bilayers. The diameter of these voids approached the average diameter of toroidal

xanthan-chitosan condensates.[10]

The height measurements by DW-RICM indicated that the build-up of chitosan-xanthan multilayers could not be sustained at low ionic strength. On the other hand, systematic studies of the surface morphology of the multilayers using AFM showed the presence of aggregates increasing in number and size with the number of bilayers. The changes observed in the AFM topographs, viewed in conjunction with the height measurements suggest that adsorbing polymer to a large extent is included in the observed islets, increasing their size without adding much to the overall thickness of the films. The probe diameter used to measure the height in DW-RICM is rather large (10 μm) compared to size of the aggregates and their separation. Thus a build-up process where the added material primarily adds to these polymer patches without adding much to their heights might not be reflected in the height measurements. With increasing number of bilayers the islets will dominate the surface, and will reduce the probability of measuring the height of the underlying network using DW-RICM. The large standard deviations in height observed for the smallest number of bilayers prepared at 5mM support the presence of aggregates as observed with AFM.

Depending on the multilayer system, a swelling response has been reported.[32, 33] This swelling of multilayer films has been attributed to uncompensated charges within the multilayers.[34] The insensitivity of the (chit_xan) multilayers to changes in ionic strength could originate from only a small fraction of uncompensated charges within the layers, or from the relatively large stiffness of the employed polymers (in particular xanthan). Due to the high persistence length of xanthan (L_p ~120 nm),[7, 9] the range of employed ionic strengths will have only minor influence on the overall xantan stiffness. As a consequence the salt concentration is expected to affect the film thickness less than what is normally observed for more flexible polymers. Swelling behaviour has been successfully observed with RICM for monolayers,[35, 36] and for a multilayer system (chitosan-alginate).[37] Therefore the lack of observed swelling for chitosan-xanthan is specific to this system and is not a consequence of insufficient accuracy of the employed experimental technique.

Conclusion

This study shows that the morphology of chitosan-xanthan multilayers is dominated by the xanthan layer morphology as observed for the first bilayer. Furthermore the formation of chitosan-xanthan multilayers depends on the ionic strength. If adsorption takes place from

low ionic strength a stable multilayer growth is not sustained, substantiated by both DW-RICM measurements and AFM imaging. At this condition there is no increase in multilayer thickness with number of bilayers and two different structural domains are observed on the surface. When a high ionic strength is used for preparation, a network structure is observed. Hence the preparation properties are important, both in terms of achieving a stable multilayer growth and to tune the morphologies of the multilayers.The evolution of poresize with the number of bilayers offers the possibility to tune diffusion properties of the system. Furthermore, biocompatibility of surfaces is related to the surface roughness.[38, 39] Both the development of a multilayer structure with a dominant network structure and the insensitivity to changes in ionic strength indicate that the high chain stiffness of xanthan is important in determining the multilayer properties.

Acknowledgements

This work is supported by The Norwegian Research Council (grants 134674/140 and 121894/420) and through the Centre for Biopolymer Engineering at NOBIPOL, NTNU (under The Norwegian Research Council grant number 145945/130). A.B. acknowledges the partly support of the Fonds der Chemischen Industrie and the SFB 563 B14. We are grateful for the chitosan sample provided by Dr. Kjell Morten Vårum, Department of Biotechnology, NTNU.

[1] M. J. Stevens, *Biophys. J.* **2001**, *80*, 130-139.
[2] H. Noguchi, K. Yoshikawa, *J. Chem. Phys.* **1998**, *109*, 5070-5077.
[3] V. A. Ivanov, M.R. Stukan, V. V. Vasilevskaya, W. Paul, K. Binder, *Macromol. Theor. Simul.* **2000**, *9*, 488-499.
[4] O.R. Rojas, M. Ernstsson, R. D. Neuman, P. M. Claesson, *Langmuir* **2002**, *18*, 1604-1612.
[5] S. T. Dubas, J. B. Schlenoff, *Macromolecules* **1999**, *32*, 8153-8160.
[6] G. Decher, *Science* **1997**, *277*, 1232-1237.
[7] T. Sato, T. Norisuye, H. Fujita, *Polymer J.* **1984**, *16*, 341-350.
[8] T. Sato, T. Norisuye, H. Fujita, *Macromolecules* **1984**, *17*, 2696-2700.
[9] M. Nakasagu, T. Norisuye, *Polymer J.* **1988**, *20*, 939-944.
[10] G. Maurstad, S. Danielsen, B. T. Stokke, *J. Phys. Chem. B* **2003**, *107*, 8172-8180.
[11] X. Shi, R. J. Sanedrin, F. Zhou, *J. Phys. Chem. B* **2002**, *106*, 1173-1180.
[12] Y. Lvov, G. Decher, G. Sukhorukov, *Macromolecules* **1993**, *26*, 5396-5399.
[13] G. B. Sukhorukov, H. Möhwald, G. Decher, Y. M. Lvov, *Thin Solid Films* **1996**, *284-258*, 220-223.
[14] G. B. Sukhorukov, M. M. Montrel, A. I. Petrov, L. I. Shabarchina, B. I. Sukhorukov, *Biosens. Bioelectron.* **1996**, *11*, 913-922.
[15] B. E. Christensen, O. Smidsrød, A. Elgsaeter, B. T. Stokke, *Macromolecules* **1993**, *26*, 6111-6120.
[16] J. J. Cras, C. A. Rowe-Taitt, D. A. Nivens, F. S. Ligler, *Biosens. Bioelectron.* **1999**, *14*, 683-688.
[17] J. Schilling, K. Sengupta, S. Goennenwein, A. R. Bausch, E. Sackmann, *Phys. Rev. E* **2004**, *69*,

[18] C. Picart, K. Sengupta, J. Schilling, G. Maurstad, G. Ladam, A. R. Bausch, E. Sackmann, *J. Phys. Chem. B* **2004**, *108*, 7196-7205.
[19] J. Schilling, *PhD-thesis,* E22 Technische Universität München, Munich, Germany, 2003.
[20] J. Schilling, E. Sackmann, A. R. Bausch, *Rev. Sci. Instrum.* **2004**, In press
[21] J. B. Schlenoff, H. Ly, M. Li, *J. Am. Chem. Soc.* **1998**, *120*, 7626-7634.
[22] P. Bertrand, A. Jonas, A. Laschewsky, R. Legras, *Macromol. Rapid Comm.* **2000**, *21*, 319-348.
[23] X. Arys, A. M. Jonas, A. Laschewsky, R. Legras, in: *"Supramolecular polymers"*, A. Cifferi, Ed., Marcel Dekker Inc., New York, 2000, pp. 505-563
[24] G. B. Sukhorukov, J. Schmitt, G. Decher, *Ber. Bunsenges. Phys. Chem.* **1996**, *100*, 948-953.
[25] D. K. Kim, S. W. Han, C. H. Kim, J. D. Hong, K. Kim, *Thin Solid Films* **1999**, *350*, 153-160.
[26] R. F. M. Lobo, M. A. Pereira-da-Silva, M. Raposo, R. M. Faria, O. N. Oliveira Jr, *Nanotechnology* **2003**, *14*, 101-108.
[27] K. Lowack, C. A. Helm, *Macromolecules* **1998**, *31*, 823-833.
[28] U. Voigt, W. Jaeger, G. H. Findenegg, R. v. Klitzing, *J. Phys. Chem. B* **2003**, *107*, 5273-5280.
[29] J.-L. Menchaca, B. Jachimska, F. Cuisinier, E. Perez, E. *Colloids Surf. A* **2003**, *222*, 185-194.
[30] B. Schoeler, G. Kumaraswamy, F. Caruso, *Macromolecules* **2002**, *35*, 889-897.
[31] F. Family, *Physica A* **1990**, *168*, 561-580.
[32] S. T. Dubas, J. B. Schlenoff, *Langmuir* **2001**, *17*, 7725-7727.
[33] R. Steitz, V. Leiner, R. Siebrecht, R. Klitzing, R. *Colloids Surf. A* **2000**, *163*, 63-70.
[34] B. Schwarz, M. Schönhoff, *Langmuir* **2002**, *18*, 2964-2966.
[35] K. Sengupta, J. Schilling, S. Marx, M. Fischer, A. Bacher, E. Sackmann, *Langmuir* **2003**, *19*, 1775-1781.
[36] A. Albersdörfer, E. Sackmann, *Eur. Phys. J. B* **1999**, *10*, 663-672.
[37] G. Maurstad, Y. A. Mørch, A. R. Bausch, B. T. Stokke, B. T. *In preparation,* **2004**
[38] U. Zimmermann, F. Thürmer, A. Jork, M. Weber, S. Mimietz, M. Hillgärtner, F. Brunnenmeier, H. Zimmermann, I. Westphal, G. Fuhr, U. Nöth, A. Haase, A. Steinert, C. Hendrich, *Ann. N. Y. Acad. Sci.* **2001**, *944*, 199-215.
[39] C. M. Bünger, C. Gerlach, T. Freier, K. P. Schmitz, M. Pilz, C. Werner, L. Jonas, W. Schareck, U. P. Hopt, P. de Vos, P. *J. Biomed. Mater. Res.* **2003**, *67A*, 1219-1227.